RECENT PROGRESS ON THE NBS PRIMARY FREQUENCY STANDARD

D. J. Glaze, Helmut Hellwig, Stephen Jarvis, Jr.
A. E. Wainwright, and David W. Allan

Time and Frequency Division
National Bureau of Standards
Boulder, Colorado 80302
Tel.: (303) 499-1000 Ext. 3207

Summary

The design of NBS-5 is discussed in detail including its relation to previous NBS primary cesium beam frequency standards. The application of pulsed microwave excitation, and the use in the accuracy evaluation of frequency shifts due to known changes in the exciting microwave power are discussed. Significant changes in the measured atomic velocity distribution with the beam alignment are reported and compared with measured Ramsey patterns. Stabilities of 3×10^{-14} for one-day averaging are reported and data on accuracy are given. Preliminary results give an evaluated accuracy of 2×10^{-13} with indications that this figure may be improved in the future.

The bias-corrected frequency of NBS-5 agrees to within 1×10^{-13} with the value obtained with NBS-III in 1969 which is preserved in the rate of the NBS Atomic Time Scale.

Key words: Cesium beam standard, Doppler effect, Frequency accuracy, Frequency stability, Power shift, Primary frequency standard.

Introduction

A primary cesium beam frequency standard serves to realize the unit of time interval, the second, in accordance with the international definition as formulated at the XIII General Conference on Weights and Measures in 1967: "The second is the duration of 9 192 631 770 periods of the radiation corresponding to the transition between the two hyperfine levels of the ground state of the cesium-133 atom". The realization of an output frequency from a real device involves several steps of physical and technical processing which may cause frequency deviations of the output frequency from the atomic unperturbed transition frequency. The magnitude of each such bias can be evaluated with the aid of experiments and of theoretical considerations. However, these biases are not known to infinite certainty. The magnitude of these uncertainties depends on the degree of theoretical understanding as well as on the precision with which experimental parameters can be measured. This precision depends on two things. One is the design and construction of the cesium beam tube and electronics of the primary frequency standard as well as on the frequency stability of the reference frequency standard used in the evaluation of the primary standard. The combined uncertainty of all biases is refferred to as the accuracy of the frequency standard.

Since the first atomic clock was realized as an ammonia frequency standard by Harold Lyons at NBS in 1948 [1], several cesium based primary frequency standards have operated at NBS. Standards[(1)] called NBS-I, NBS-II, and NBS-III served successively as primary frequency standards during the 1950's and 1960's [2, 3]. NBS-III, our previous operating frequency standard, was evaluated in 1969 to an accuracy of 5 parts in 10^{13}. [3]

The experience gained with NBS-III indicated that the main limitations for accuracy, in addition to significant electronics problems, were the magnetic field--in particular its homogeneity and stability--the second-order Doppler effect, and the cavity phase difference (large for NBS-III). Therefore the design and construction of a new primary cesium beam frequency standard with the designation NBS-5 was initiated with features incorporated to significantly reduce the above-mentioned limitations.[(1)] The instrument was designed to achieve a frequency accuracy of 1 part in 10^{13}. To facilitate accuracy evaluations, the design also aimed at greatly increasing the frequency stability which is basically given by the available atomic beam intensity and the resonance line Q. The stability for 1 hour sampling time of NBS-III was 2 parts in 10^{13}. The NBS-5 design aimed at improving this value by at least one order of magnitude, thus allowing measurement precisions approaching 10^{-14} within 1 hour. NBS-5 was put into operation during the latter part of 1972, and has undergone several phases of accuracy evaluation.

The NBS-5 System

A photographic view of NBS-5 with all electronics is depicted in Fig. 1. For comparison, a photograph of NBS-III is shown in Fig. 2. The complete NBS-5 system has a length of about 6 m overall. The vacuum system is basically a stainless steel tube, 25 cm in diameter, and is evacuated by three 200 ℓ/s ion pumps which can be closed off with valves for servicing.

Figure 3 gives a schematic view and a comparison of the beam alignments in NBS-5 and NBS-III. In contrast to the NBS-III design, a beam stop at the exit of the first NBS-5 magnet is used to reduce background due to fast atoms reaching the detector along the line of sight. This location for the beam stop gives both maximum filtering of fast atoms with minimal effect on slower atoms and minimum cesium deposition on

(1) Another cesium beam frequency standard with the designation NBS-X4 was also constructed in cooperation with Hewlett-Packard Company. This device, however, was not originally designed to be used as a primary cesium beam frequency standard. New techniques, however, coupled with its expected high stability, should permit its use as an accurate standard. [9, 10] NBS-X4 will likely be of great use to measurements involving both the NBS Atomic Time Scale and the evaluation of NBS-5.

the inner walls of the cavity. Such deposition can lead to variable phase difference between the interaction regions and to attendant frequency fluctuations[3]. Also indicated in Fig. 3 are the two limiting trajectories of the highest and lowest velocities which successfully reach the detector. The trajectories shown originate from collimator channels along one edge of the collimator assembly. In the drawing, it is assumed that transitions are induced in the cavity region which cause a change of state in all the atoms. The figure gives the trajectories of useful (2) atoms leaving the oven on only one of the two atomic states which participate in the transition. The other state is also utilized and has corresponding trajectories, starting below the optical axis of Fig. 3, and then crossing over at the center aperture of the tube. The center aperture thus is reasonably well located at the crossover of the trajectories of all velocities for the two states.

The cavity and magnetic shield structures are shown schematically in Fig. 4. The basic C-field design is similar to that of NBS-X4 and is attributable to and patented by Lacey et al., Hewlett-Packard Co.[4]. The cavity and magnetic shields are located inside of the vacuum system in order to assure mechanical stability and to prevent thermal effects. The length of the Ramsey-type cavity is 3.74 m. One of the most critical parameters of the beam tube is the phase difference between the two interaction regions of the cavity. For the first time at NBS, this parameter was carefully trimmed before assembly of the tube. The trimming was done by separate measurements of the cavity components: interaction regions, arms, and E-plane tee. The testing and further corrective actions continued during the assembly of these cavity components. The electrically measured cavity phase difference was less than 1 mrad at the time of final assembly. This phase difference has not been adjusted (and indeed cannot be adjusted) since the assembly of NBS-5.

The magnetic shield package consists of three separate magnetic shields: two of a box-like structure containing the microwave cavity; the third outer shield of a cylindrical design. The shields, microwave cavity, and vacuum system are all electrically insulated from one another except at the center of the beam tube where all are joined at one point which is the system ground. Figure 5 depicts a photographic view of the structures before assembly. The typical operating field is about 60 milli-oersted, and a field homogeneity of better than 1% peak-to-peak along the tube axis was measured with a field probe after assembly.

The deflection magnets are shown in Fig. 6. They have a length of 35 cm and a gap of 1.2 cm (measured at the center). The pole-tip configuration reproduces a two-wire field, and the peak field strength at the pole tip is about 9.3 kG. Trimmers are located on the cavity side of the magnets and are carefully adjusted to assure a smooth transition (in strength as well as orientation) from the high magnetic field of the magnet through the magnetic shield end caps into the shielded cavity region, thus avoiding Majorana effects. The beam tube permits an atomic beam to traverse the path through the cavity in either direction. Each end of the beam tube is equipped therefore with both identical magnets and oven-detector combinations. For beam reversal the beam stop, shown in Fig. 3, can be withdrawn and a second beam stop can be inserted at the other magnet. This capability of beam reversal was introduced in order to provide the system with an additional measurement capability of the cavity phase difference bias: the frequency bias changes sign if the beam traverses the cavity in the opposite direction. The oven-detector combination, depicted in Fig. 7, is arranged in such a way that it can be adjusted in the deflection plane of the atomic beam, perpendicular to the beam axis; in addition, the oven can be aimed independently at different angles. The oven can accept ampules filled with 5 g or more of cesium which yield a projected lifetime of more than a year continuous operation. The collimator of the oven is an array of about 500 separate channels producing a beam with a rectangular cross section of 2 mm × 9 mm. With an oven temperature of 100° C, the projected beam intensity at the detector is approximately 10^8 atoms per second. The detector is a platinum ribbon. Because of the relatively high beam intensity and the high purity of the platinum ribbon (total background current is of the order of 0.1 pA), no mass spectrometer and electron multiplier are employed. Instead, a field effect transistor is mounted in close proximity to the detector. The detector signal is processed in low-noise preamplifiers external to the beam tube. If one end operates in the "oven" mode the detector is moved aside; however, if the end is used in its "detector" mode, the detector can move in front of the oven and, at the same time, a carbon getter plate baffles the oven collimator (see Fig. 7). Lowering the oven temperature to approximately room temperature at this end also reduces its output.

The microwave signal is obtained from a crystal oscillator at a basic frequency of 5,006,880 Hz, a subharmonic of the cesium transition frequency. As shown in Fig. 8, an associated low noise multiplier chain which drives a step recovery diode produces a signal at the cesium atom resonance frequency with a power of up to 20 mW. The older klystron and primary loop phase-lock systems [3] have now been eliminated, and all systems are now redesigned with solid state components. Phase noise measurements for these new multiplier systems are shown in Fig. 3 of Ref. 3. A sinusoidal frequency modulation can be applied with a fundamental frequency of 18.75 Hz. This modulation is generated with second-harmonic suppression of better than 100 dB. The modulation reappears in the beam current at the detector, is amplified, phase detected, and processed in two cascaded integrators and used to servo-control the crystal oscillator. (The original idea and design for the double integrator was first proposed by Cutler at Hewlett-Packard Co.[5].) The 5,006,880 Hz crystal oscillator frequency is also separately synthesized to a standard 5 MHz frequency. This signal is used for evaluative and stability measurements, and for time scale calibrations.

(2) Useful atoms are those which both undergo the $(F=4,\ m_F=0) \longleftrightarrow (F=3,\ m_F=0)$ transition and reach the detector.

Preliminary Experimental Results
(Status May 1973)

After a preliminary beam alignment, the $(F = 4, m_F = 0) \longleftrightarrow (F = 3, m_F = 0)$ transition was observed with peak-to-valley amplitude of 4 pA. Since the atomic velocities are determined by the beam optics and the beam alignment, linewidths of 25 to 45 Hz were measured depending on the alignment. The signal-to-noise ratio was also measured and from this, by Lacey's method[6], the frequency stability for 1 s sampling times was calculated to be 4 parts in 10^{13}. Our best reference sources in stability measurements for very short times were crystal oscillators, and for longer times were commercial cesium beam frequency standards. A plot of the measured square root of the Allan variance using both of these reference oscillators is shown in Fig. 9 together with the calculated stability of NBS-5. Figure 9 shows that we were able to obtain measurement precisions in the accuracy evaluation of about 3 parts in 10^{14} for sampling times of 10^5 s. The calculated, shot noise limited stability is better than the measured performance. This is due to limitations in the electronics; i. e., due to noise associated with the 5,006,880 Hz quartz crystal oscillator. In the long-term measurements, the available commercial cesium reference was also limiting the measurement precision.

At the time of this writing, for various technical reasons, we have not yet completed beam reversal experiments. However, we have experimentally established that in the "detector-mode" (with an opened Cs-ampule in the oven) the background current is only a fraction of a picoampere.

The following report on accuracy data is based on two other evaluation methods:

(1) Power shift measurements[7-10]. This method is based on the fact that the effective mean atom velocity is a function of the interrogating microwave power. To use this method it is necessary (a) to know the velocity distribution in the tube (this can be obtained experimentally from pulsed operation [see below] and refined by matching a derived Ramsey spectrum with the experimentally obtained Ramsey spectrum). (b) to calculate numerically the effective mean velocities at given microwave power settings, and (c) to measure the change in the output frequency by comparison with a reference standard at different microwave power settings. This allows a calculation of the cavity phase difference and the corresponding frequency bias. It must be verified that the microwave spectrum is of sufficient purity so as not to introduce spectrum-related power shifts.

(2) Pulse method[9, 10]. This method is based on selecting certain velocities in the beam by pulsing the microwave power. The velocity selection is based on the time of flight between the two cavity interaction regions. This method also allows a measurement of absolute microwave power levels in the cavity and the determination of the velocity distribution.

With methods 1 and 2 we measured the biases due to the second-order Doppler effect and the cavity phase difference. We have monitored these values every month during the first three months of 1973. We could not find any change in the cavity phase shift within our measurement precision. Our results are tabulated in Table 1. The results (bias at optimum power) show a remarkable consistency. If we pool all power shift data, we obtain for the bias at nominally optimum power (sinusoidal modulation of 21 Hz amplitude):

$$(-14.5 \pm 1.6) \times 10^{-13}.$$

This pooling assumes, of course, that NBS-5 parameters in reality did not change, and all changes in the individual data are random, uncorrelated [11] The pulse method result agrees with the above value to within the uncertainty estimates. In Table 2 we list, together with the above value (item 1 in Table 2), all other known biases and bias uncertainties. No listing in the bias column indicates that the most probable bias value is zero. If all values are treated as uncorrelated data, the combined bias uncertainty is 2×10^{-13}. (Square root of the sum of the squares).

As was mentioned above, the velocity distribution of NBS-5 had to be known in order to carry out the accuracy evaluation. Figures 10 and 11 show two velocity distributions of NBS-5 for different beam alignments measured by the pulse method [9, 10]. The normal, on-axis alignment is depicted in Fig. 10. The distribution has a Maxwellian characteristic with high and low velocity cutoffs. The alignment was changed a few millimeters to an off-axis alignment of oven and detector, producing a distribution as depicted in Fig. 11. The low velocity cutoff is not much different from the one in Fig. 10; however, the distribution shows two distinct peaks. We interpret these two peaks as belonging to the two atomic states which are used in the tube. For an on-axis alignment the trajectories of the two states are reasonably symmetric with respect to the tube axis and thus contain approximately the same velocities. In the off-axis alignment this symmetry is no longer present; the trajectories-- and the corresponding velocity cutoffs-- may be different to a considerable extent. The two states with their two different sets of trajectories thus contain different velocity distributions, and Fig. 11 is a composite of two distinct distributions.

The velocity distribution is directly reflected in the Ramsey pattern [7-10]. Figure 12 shows a set of patterns corresponding to the velocity distribution of Fig. 10. The patterns at optimum power as well as those at higher and lower microwave power show a smooth, similar characteristic. The major differences are a change in the linewidth (and period of the pattern) corresponding to the selection of lower velocities at low power and higher velocities at above optimum power. The two-peak distribution of Fig. 11 is reflected in the corresponding Ramsey patterns of Fig. 13 which show, in particular at above and below optimum power, a distinct interference structure between two patterns of different period due to the two velocity peaks.

Conclusions

The above data show that we obtained an accuracy evaluation with a 1-sigma uncertainty of 2×10^{-13}. We note that all other bias uncertainties are likely to be negligible as compared to the reported second-order Doppler and cavity phase-shift bias uncertainties. The results reported here ought to be regarded as tentative, preliminary values, subject to later verification and/or correction. For the future we plan to understand fully the beam optics alignment and the magnetic field properties of the beam tube. In addition, we expect to compare the computer aided beam optics design with actual performance. The pulse method and the power shift method have been used successfully in the accuracy evaluation and we would like to emphasize their potential utility in cesium beam tubes of almost any design. However, final confirmation of the data by successful beam reversal experiments remains our objective.

Only after all these tests are completed do we feel that final accuracy figures can be quoted for NBS-5. Further improvements in accuracy seem likely in view of new ideas and evaluative methods for NBS-5, and in view of the beam tube performance to date. In addition, the availability of an accurate and very stable reference standard (i. e., NBS-X4) is expected to facilitate evaluation of NBS-5 and to lead to further improvements in accuracy.

In conclusion, it is interesting to note that the frequency of NBS-5, with the bias corrections of Tables 1 and 2 applied, agrees with the bias-corrected frequency of NBS-III[3] during the summer of 1969 to within 1×10^{-13} as seen through the NBS Atomic Time Scale.[11]

Also, at the time of this writing, the agreement between several national standards as compared via the International Atomic Time Scale (TAI) is quite excellent as can be seen from Table 3. The agreement among the values of Table 3 is well within the individual accuracy claim of each individual measurement. This is quite satisfying for everybody involved in primary frequency standards and time scale work.

TABLE 1
Results of Power Shift Measurements

Date of Experiment	relative to optimum power P_H (nominal values)	P_L	measured $\nu_H - \nu_L$	uncertainty	δ	bias $\nu - \nu_{cs}$	bias at nominal optimum power	bias uncertainty
27-31 Jan 73	+4 dB	-6 dB	-3.46×10^{-13}	0.3×10^{-13}	0.71 mrad	-15.6×10^{-13} (at + 4 dB)	-15.0×10^{-13}	3×10^{-13}
12-15 Feb 73	+4 dB	-8.6 dB	-3.66×10^{-13}	0.3×10^{-13}	0.65 mrad	-15.4×10^{-13} (at + 4 dB)	-14.2×10^{-13}	2×10^{-13}
17-23 March 73	+4.5 dB	-9 dB	-3.1×10^{-13}	0.7×10^{-13}	0.71 mrad	-15.4×10^{-13} (at +4.5 dB)	-15.0×10^{-13}	5×10^{-13}
Result of pulse method measurement.								
24 March - 2 April 73	pulse period T_H=14 ms	T_L=22 ms	-4.7×10^{-13}	1.2×10^{-13}	0.55 mrad	--	-12.8×10^{-13}	2.5×10^{-13}

TABLE 2

Preliminary Accuracy Budget for NBS-5

	Influencing Factors	Bias	Bias Uncertainty
1.	2nd-order Doppler and phase difference at nominal optimum power; source: power shift & pulse method	-14.5×10^{-13}	1.6×10^{-13}
2.	servo system; source: some variation of servo parameters and calculations based on measured offsets and loop gain	---	1×10^{-13}
3.	magnetic field; source: $m_F \neq 0$ transitions	$1,670.0 \times 10^{-13}$	0.2×10^{-13}
4.	$\overline{H^2}$ versus $\overline{H}^2$; source: $m_F \neq 0$ transitions and measurements during assembly (no correction is applied, the bias is the uncertainty)	---	0.4×10^{-13}
5.	Majorana transitions; source: $m_F \neq 0$ transitions and measurements during assembly	---	0.05×10^{-13}
6.	pulling of neighboring lines; source: $m_F \neq 0$ transitions	-0.05×10^{-13}	0.02×10^{-13}
7.	cavity pulling; source: worst estimate	---	0.1×10^{-13}
8.	rf spectrum; source: spectrum recording	---	0.4×10^{-13}
9.	random uncertainty (1σ at 10 h); source: stability measurements against other cesium standards	---	$<0.4 \times 10^{-13}$

TABLE 3

Fractional frequency difference, $\frac{\Delta\nu}{\nu}$, between the International Atomic Time Scale (TAI) and the individual standard

Standard	$\frac{\Delta\nu}{\nu}$ (rounded)	Reference	Year
NBS-III [3]	$+ 10 \times 10^{-13}$	3	1969
PTB-Cs1	$+ 12 \times 10^{-13}$	12	1973
NRC-Cs5 [4]	$+ 10 \times 10^{-13}$	13	1973
NBS-5 [3]	$+ 12 \times 10^{-13}$	11	1973

[3] Includes relativistic frequency correction due to altitude.

[4] This value is based on the frequency of Cs 5 from a relatively short comparison (12 days in February 1973) between Cs 3 and Cs 5 (preliminary evaluation) of NRC. The relationship between Cs 3 and TAI was known from measurements extending over many months.

Acknowledgments

The authors wish to express sincere appreciation for the help of the late J. H. Holloway for many helpful discussions regarding beam optics design and other problems associated with cesium beam tubes. His continued interest and support over several years have contributed very significantly to the success of this present work.

L. S. Cutler has contributed significantly to the NBS-5 work in the areas of beam optics and electronics (especially on the double integrator and servo system) and the authors appreciate his considerable help.

We wish also to thank L. F. Mueller for his extensive help during the final assembly phase of NBS-5.

The authors wish to thank J. A. Barnes and Donald Halford for their help and encouragement throughout many phases of the work on NBS-5. We also appreciate the efforts of W. D. McCaa, Jr., during the latter phase of the work and the efforts of H. F. Salazar on the diagnostic electronic systems. The work of C. S. Snider who helped on mechanical design and testing of the reversible beam system is also appreciated.

A special word of commendation should be given to Ward T. Roberts who constructed almost all of the NBS-5 beam tube. His careful work, continued enthusiasm, and contributions to the design over several years, have had a significant impact on the success of this work.

Finally, the authors wish to thank Patsy J. Tomingas and Carol J. Wright for their efficient preparation of this manuscript.

References

1. H. Lyons, Ann. N. Y. Acad. Sci., 55, pp. 831 871 (1952).

2. R. E. Beehler and D. J. Glaze, IEEE Trans. Instrum. and Meas., IM-15, No. 1 and 2, pp. 48-55 (1966)

3. D. J. Glaze, IEEE Trans. Instrum. and Meas., IM-19, No. 3, pp. 156-160 (1970).

4. R. F. Lacey, L. S. Cutler, and W. F. Turner, U. S. Patent No. 3670171.

5. L. S. Cutler, private communication.

6. R. F. Lacey, A. L. Helgesson, and J. H. Holloway, Proc. IEEE, 54, No. 2, pp. 170-176 (1966).

7. H. Hellwig, J. A. Barnes, D. J. Glaze, and P. Kartaschoff, Nat. Bur. Stand. (U. S.) Tech. Note 612 (February 1972); also H. Hellwig, J. A. Barnes, and D. J. Glaze, Proc. 25th Ann. Symp. on Frequency Control pp. 309-312 (1971).

8. A. G. Mungall, Metrologia, 8, pp. 28-32 (1972).

9. H. Hellwig, S. Jarvis, D. Halford, and H. E. Bell, Metrologia, 9, No. 3 (July 1973)

10. H. Hellwig, S. Jarvis, D. Halford, and H. E. Bell, Proc. 27th Ann. Symp. on Frequency Control (1973).

11. D. W. Allan, D. J. Glaze, H. E. Machlan, A. E. Wainwright, and H. Hellwig, Proc. 27th Ann. Symp. on Frequency Control (1973).

12. G. Becker, private communication, to be published, 1973.

13. A. G. Mungall, private communication; also A. G. Mungall, R. Bailey, H. Daams, D. Morris, and C. C. Costain, Proc. 27th Ann. Symp. on Frequency Control (1973).

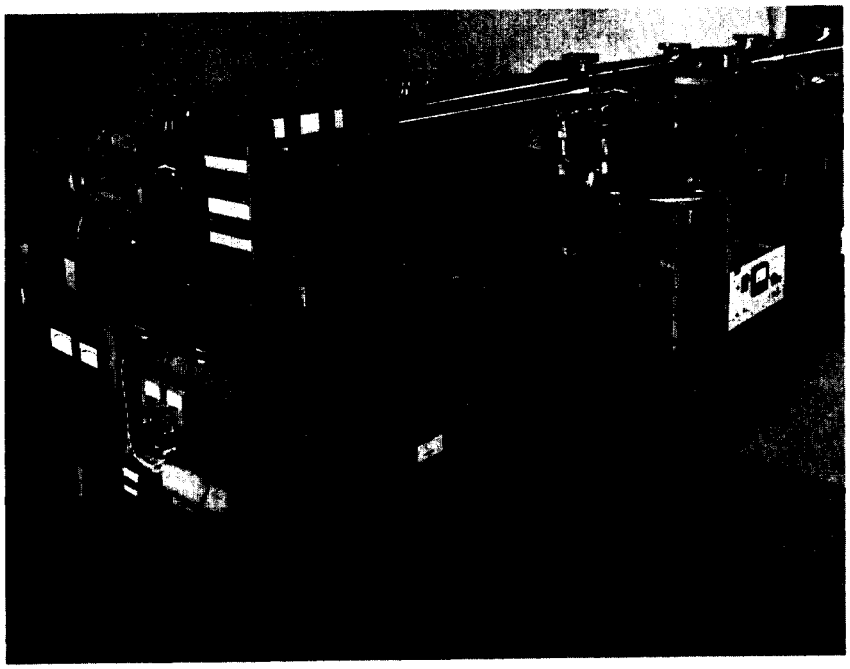

Figure 1. View of NBS-5. All electronics systems are shown.

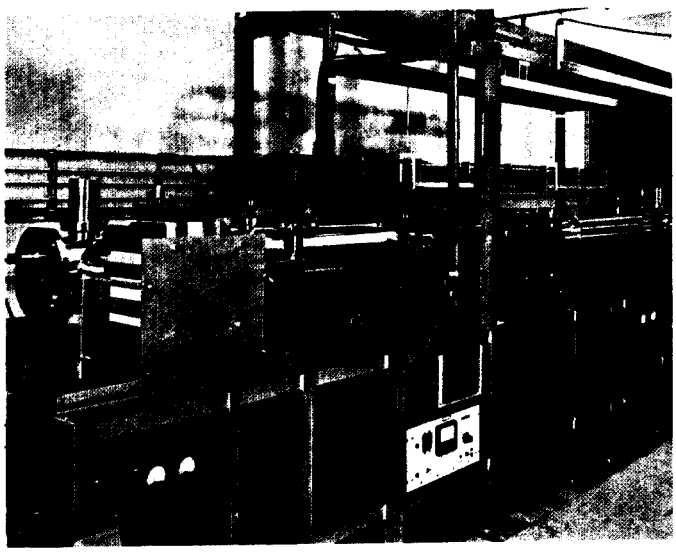

Figure 2. View of NBS-III. Frequency lock electronic systems are not shown.

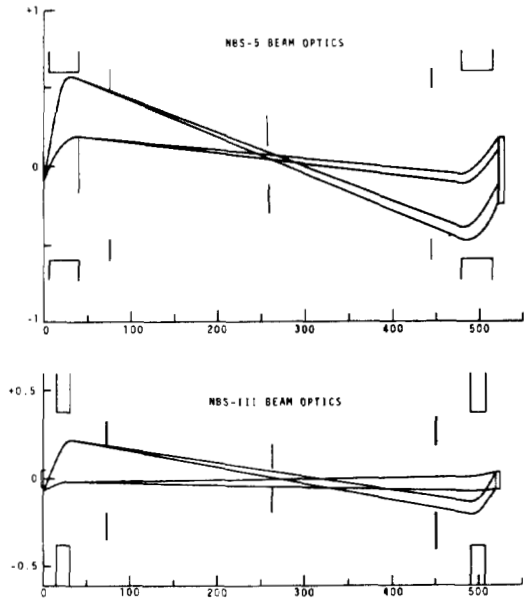

Figure 3.

Beam optics comparisons of NBS-5 and NBS-III. Scales are in cm. Cavity and center slit apertures together with the NBS-5 beam stop are designated by vertical lines. The magnet gaps are represented by unclosed rectangles, while detectors are shown by closed rectangles. The collimator for NBS-5 is a series of dots, while the uncollimated source for NBS-III is an unclosed rectangle.

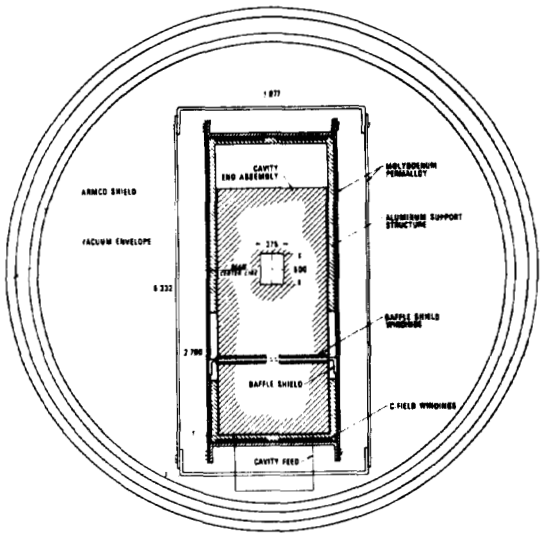

Figure 4.

Cross section scale drawing of NBS-5 Beam Tube. Dimensions are in inches. The cavity structure, aluminum support structure, and magnetic shields are all electrically insulated from one another except at the cavity feed. There they are all joined electrically to one point which is the system ground. The baffle shield (and its windings) serve to shield the beam from the opening through which the cavity feed passes. The baffle shield and its windings are approximately 76 cm in length. The innermost rectangular molybdenum-permalloy shield and windings define the C-field region of 427 cm in length.

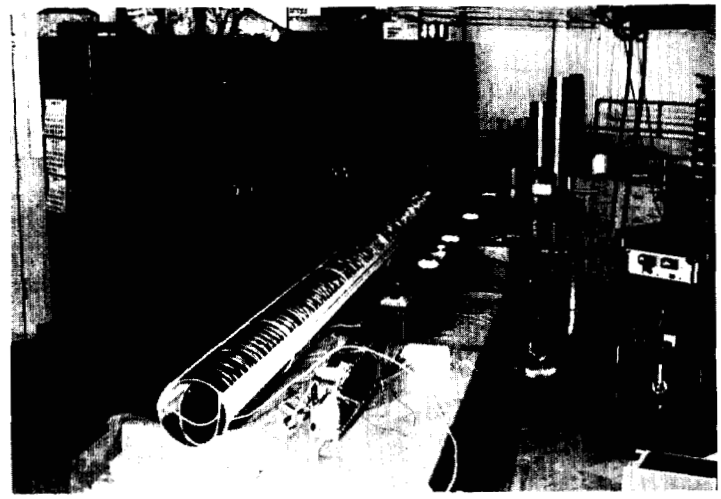

Figure 5.

View of the microwave cavity/magnetic shield package before final assembly. The cylinder on the left is the outer shield, the box-like structure on the right comprises the two inner shields and contains the microwave cavity.

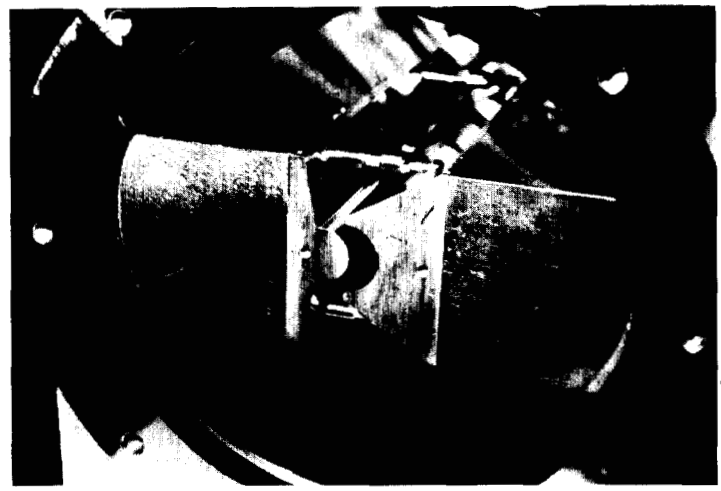

Figure 6.

View of one of the dipole magnets. Gap-width 1.2 cm. Pole tips and return ring are soft iron; magnetic drivers, between pole tips and return ring, are alnico-5.

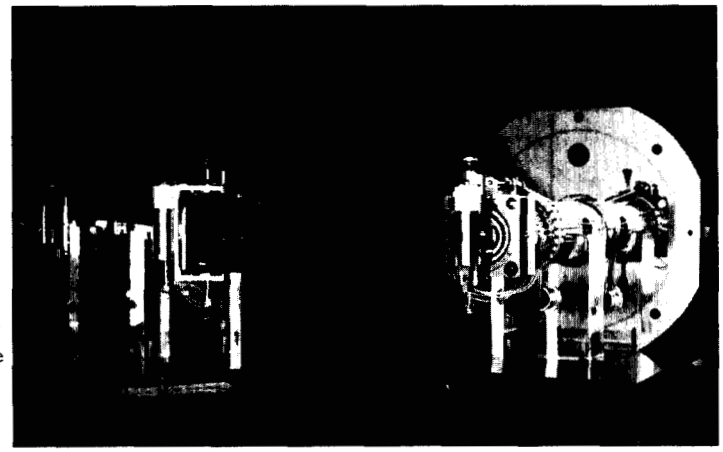

Figure 7.
View of the oven/detector combination of both ends of the tube before final assembly. The system on the left is adjusted for the "oven-mode", the one on the right for the "detector-mode".

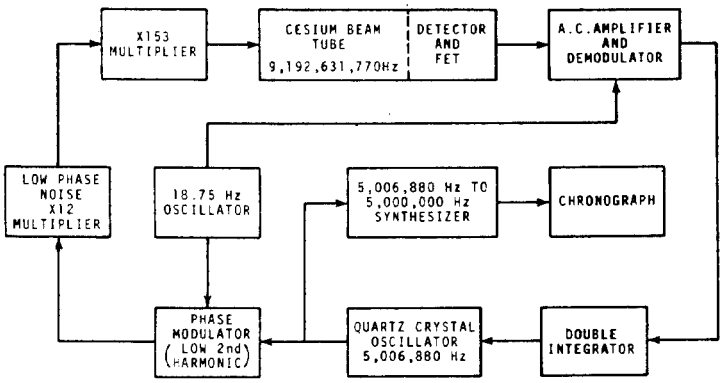

Figure 8.

Block diagram of the NBS-5 electronics system. All components are now solid state. Phase noise measurements for the frequency multiplier are described in [3].

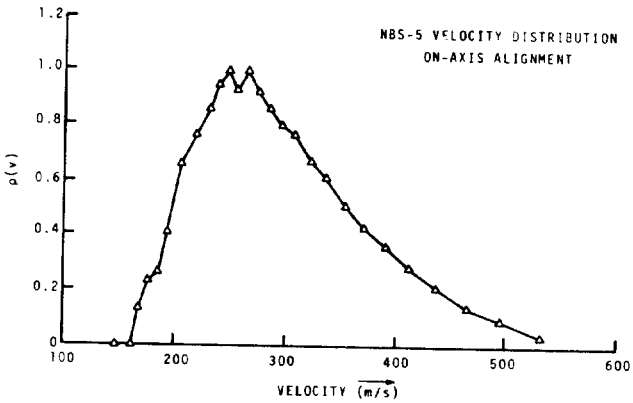

Figure 10.

Velocity distribution of NBS-5; on-axis alignment. Measured by the pulse method [9, 10]; velocity window: approximately 10%.

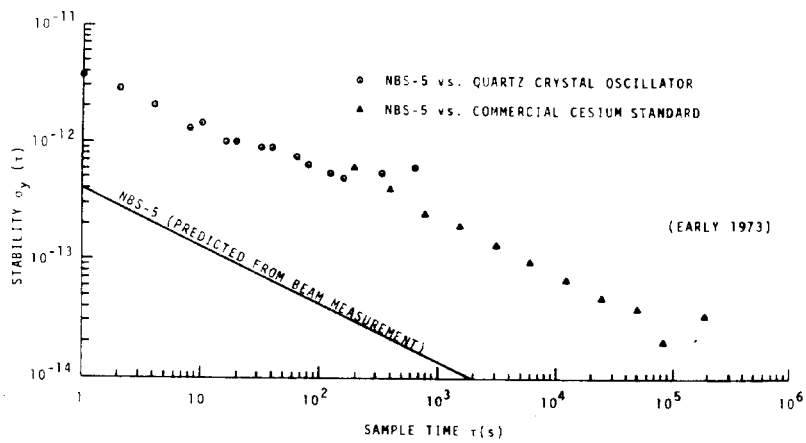

Figure 9.

Measured and calculated frequency stability of NBS-5.

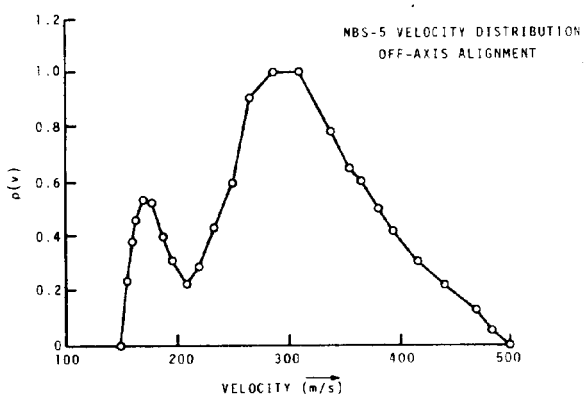

Figure 11.

Velocity distribution of NBS-5; off-axis alignment. Measured by the pulse method [9, 10]; velocity window: approximately 10%.

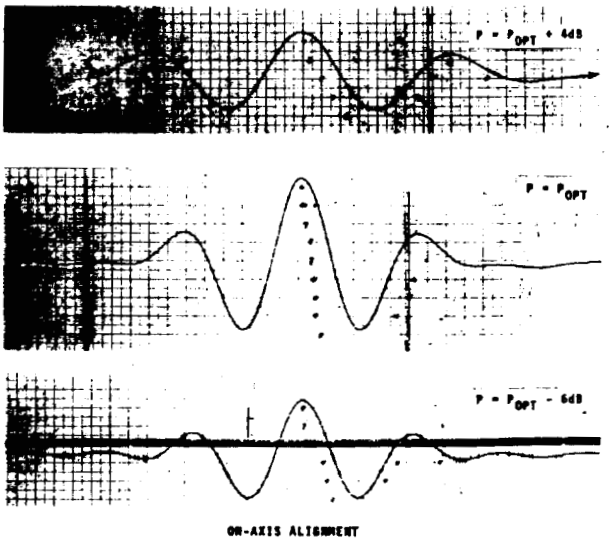

Figure 12. Ramsey pattern corresponding to Fig. 10 at three different power settings (P_{opt} = optimum power). Vertical and horizontal scales identical for all three curves. Horizontal scale unit: 12 Hz/major division; recording time constant: 1 s; sweep speed: 1Hz/s.

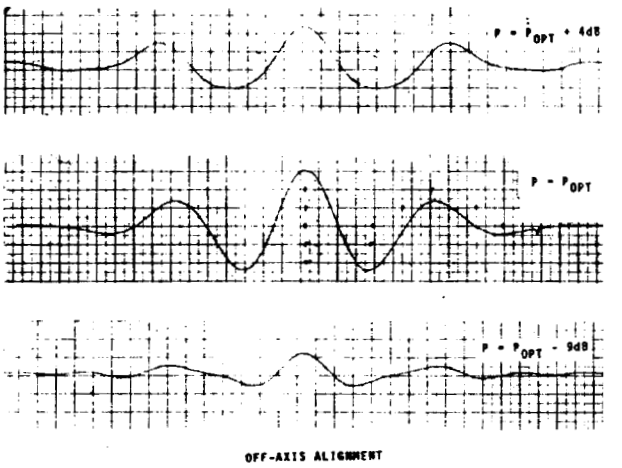

Figure 13. Ramsey pattern corresponding to Fig. 11 at three different power settings (P_{opt} = optimum power). Vertical and horizontal scales identical for all three curves. Horizontal scale unit: 12 Hz/major division; recording time constant: 1 s; sweep speed: 1 Hz/s.